EFFECT OF PROCESSING AND LOADING CONDITIONS UPON THE FATIGUE BEHAVIOUR OF A C_f/EPOXY LAMINATE

Christos Koimtzoglou[1,3], Konstantinos G. Dassios[2,*] And Costas Galiotis[1,2]

[1] Foundation for Research and Technology Hellas, Institute of Chemical Engineering and High Temperature Processes, Stadiou Street, Platani, Patras GR-26504, Greece
[2] Department of Materials Science, University of Patras, Rio GR-26500, Greece
[3] Integrated Aerospace Sciences Corporation, 17 Tegeas Street, Argyroupolis, GR-16452, Greece

*Author to whom correspondence should be addressed,
E-mail: kdassios@iceht.forth.gr

ABSTRACT

The current work reports on the tensile and fatigue behaviour of an autoclave-cured unidirectional carbon fibre reinforced epoxy-matrix laminate. The macromechanical properties of the composite are established under interrupted and uninterrupted, static and dynamic conditions at a maximum strain below the critical fatigue limit of the matrix material. The established S-N curve was used to calculate the endurance fatigue limit of the laminate as well as to record an increase in fatigue life of specimens tested at load levels lower than two standard deviations below the mean static strength of the material. The failure modes exhibited by the composite under all testing conditions were recorded and interpreted by means of the damage mechanisms that originate them. The results of interrupted testing showed that the combined effect of fatigue and residence at high stress levels for prolonged periods of time - conditions that simulate a realistic loading scheme- trigger premature fibre failure and thus specimen failure.

Keywords: carbon fibre, fatigue, mechanical testing, autoclave

1. INTRODUCTION

Over the last decades, polymer matrix composites have been replacing metals and other conventional monolithic materials in a growing number of load-bearing applications such as those encountered in transportation. The most frequent cause of failure of such structures has been known to be the failure of the constituent materials as a result of fatigue [ ]. On the other hand, design of composite structures has traditionally relied mostly on the static and impact performance of these materials, while the prediction of their fatigue life has been given much less attention. Little information is available as to how the failure modes of the constituent materials interact with each other and induce areas of stress concentration that may, in turn, affect the integrity of a component [,]. For example, fibre fracture and consequent recoiling resulting from fatigue loading may initiate interfacial damage, which can propagate either as a conical shear crack or as a fibre/matrix debonding and affect the local stress transfer efficiency of the system [, ,]. Such stress redistribution may at some point trigger macromechanical damage and therefore a careful control of the initial conditions of failure can delay or accelerate the catastrophic failure of the composite [2].

The main reason for this lack of knowledge is the complexity associated with understanding the microscopic failure processes developing during fracture of a composite material, which differ from global scale phenomena. In general, the fatigue behaviour of such materials is controlled by the propagation of damage and the interaction between the various interfaces and internal boundaries which separate the dissimilar constituent materials (matrix, fibres) or building blocks (laminae) and which respond differently under dynamic loading conditions. Presently, the ultimate design strain levels are kept low, in the region of 4000 $\mu\varepsilon$, where composite materials can withstand large numbers of fatigue cycles without failing. However, to use composite structures to their full potential and to develop materials more resistant to fatigue, it is essential that the effects of various damage mechanisms on fatigue life are understood. In other words, we need to build bridges between damage/failure micro-mechanisms and fatigue life.

The distribution of stresses in the reinforcing fibres of the composite as a result of time-variable loading have a major influence on the damage modes that develop in a composite material, and therefore on the resulting state of stress at any given point in time. In a previous pilot study [ ], the micromechanics of tension–tension fatigue loading in model single-carbon-fibre composite geometries were investigated using the technique of Laser Raman Microscopy (LRM) to capture the stress state of the fibres at the microscale. Axial stress distributions and interfacial shear stress (ISS) distributions were established at various fatigue levels, and were used to obtain important parameters such as the maximum ISS the system can accommodate, the transfer length for efficient stress built-up and the length required for the attainment of maximum ISS. In the current study, coupons of full unidirectional laminates processed via the autoclave route using the same constituents (matrix, fibres) as in the model composites, are subjected to cyclic loads at a maximum strain below the critical fatigue limit of the matrix material (0.5% strain for epoxy matrices), in order to assess the initiation and evolution of damage in the fibres and the fibre/resin interface. The micromechanics of stress transfer efficiency of the composite were independently assessed by application of the LRM technique directly at the microscale during fatigue testing of the material [ ].

Herein, the processing route and properties of the carbon fibre (Cf) - epoxy resin composite system are presented and the mechanical performance of the composite material is established under both uninterrupted and interrupted testing conditions. As fatigue loading of structural parts is an anharmonic sequence of alternating loads that can pause and resume, interrupted fatigue can simulate the loading scheme encountered in a number of applications much more realistically than conventional fatigue. The study reports the static mechanical properties such as static strength, elastic modulus and failure strain of the laminate as well as its fatigue life parameters such as the S-N curve, endurance fatigue limit and residual properties. Additionally, the failure mode of the composite under both tensile and fatigue loading conditions is established and related to the effect of interruptions in the loading procedure.

2. EXPERIMENTAL

2.1. Materials & Processing

Unidirectional 8-ply composite laminates were manufactured from carbon fibre prepreg sheets under vacuum-assisted thermal processing/polymerization in a semi-industrial autoclave furnace (Aeroform Industrial Controls Ltd., UK). The prepreg material, supplied by ACG (Advanced Composites Group, UK), consisted of unidirectional M40-40B high modulus carbon fibres (Toray) in the EF2600 epoxy matrix which is in fact a higher viscosity variation of the Epikote 828 resin (Shell Chemicals).

Prepreg sheets of dimensions 300 mm x 230 mm were stacked on a polished die steel tool while an aluminium sheet was placed on top of the last prepreg layer to provide a smooth outer surface of the resulting plate. The preform was covered with several layers of breather material that collected excess resin flow during polymerization. A vacuum bag was built around the stacked sheets to enable removal of entrapped air during polymerization and to facilitate densification of the sheets.

Thermal treatment of the vacuum-bagged laminate was performed at a temperature of 120oC under a constant pressure level of 6 bar that assisted in the consolidation of the prepreg sheets and as well as in avoiding air entrapment (Fig. 1).

The quality of the resulting plates was investigated with the help of a C-Scan ultrasonic apparatus. As shown in Fig. 2, brighter areas correspond to higher levels of densification of the composite constituents

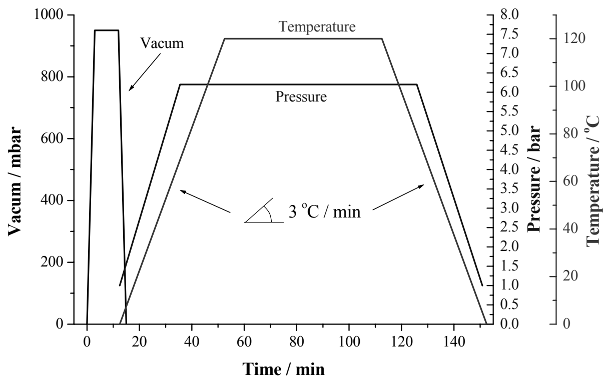

Fig. 1: Autoclave cure cycle for the M40-40B/EF2600 prepreg laminates

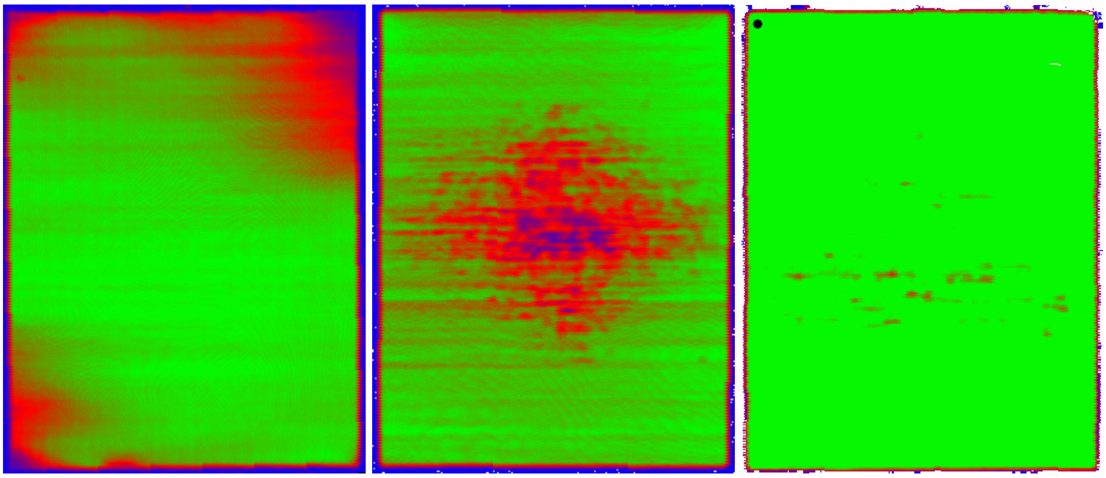

Fig. 2: C-Scan pictures of the quality of different plates processed within the context of the current work.

while dark regions indicate the existence of imperfections, local air entrapment or partial delamination. Laminates having a satisfactory densification level within their central 80% area were approved and used for the preparation of specimens, while imperfect plates were rejected.

The fibre volume fraction in the laminates after the curing was measured to ca. 65%. The fully-densified areas of the resulting [0]8 composite plates were cut according to ASTM D 3039M-95a and ASTM D 3479M-96 to produce rectangular specimens intended for static (tensile) and fatigue loading, respectively. Following the directives in the same protocols, $[+45/-45]_2$, glass-fibre reinforced polyester tabs were attached on the upper and lower edges of the specimens to improve the stress transfer efficiency at the gripping area of the specimens. The tabs were fastened on the specimens using a commercial 2-component epoxy adhesive, while a subsequent 24h curing cycle at 40 ^oC allowed the full polymerization of the glue. A summary of material dimensions is given in Table 1.

2.2. Testing

The specimens were used to perform tension and fatigue tests according to ASTM D 3039M-95a and ASTM D 3479M-96, respectively. Static tensile testing was performed for the determination of the mechanical properties of the material while fatigue loading aimed in the establishment of the S-N curve and the identification of the endurance fatigue limit of the material was also undertaken. Additional tests under static and dynamic loading were performed where the loading procedure was frequently interrupted in order to investigate the effect of combined fatigue and residence at high loads on the life of the material.

2.2.1. Tensile testing

Static tensile loading was performed on twelve (12) M40-40B/epoxy specimens in order to establish the mechanical properties of the composite material produced. The tests were performed on a MTS® 858 Mini Bionix hydraulic frame under crosshead displacement control with a rate of 1 mm/min [ASTM D 3039/D 3039M-95a]. Strain was measured using

Table 1: Dimensions of materials and specimens

Material	**Length**, mm	**Width**, mm	**Thickness**, mm
Prepreg sheet	230	300	0.25
Plate $[0]_8$	230	300	1
Specimen	230	12.7	1
Tab	57	12.7	3

strain gauges of a gauge factor of f_g = 2.1 (Kyowa KFG-5-120-C1-11L1M2R) as well as with the inherent calibrated external extensometer (MTS® Extensometer - Axial Mod.632.24F-50 Monotonic). Strain gauges were used in ten (10) specimens with the extensometer used in parallel during four (4) of them, while strain was recorded exclusively by the extensometer in two (2) tests. The determination of the elastic modulus was based on the stress-strain data in the 0.001-0.003 strain range (Tensile chord modulus of elasticity, ASTM D 3039/D 3039M-95a).

2.2.2. Fatigue

Fatigue loading was performed on fourteen (14) specimens in order to establish the S-N curve and to identify the endurance fatigue limit of the produced composite. Testing was performed on the same frame under load control conditions. The imposed loading waveform was sinusoidal with a frequency of 10 Hz and loading ratio (minimum/maximum applied load) R = 0.1 according to ASTM D 3479/D 3479M-96. The maximum applied load values used ranged from 0.62 to 0.92 of the static strength of the composite material. The specimens that endured 10^6 loading cycles were subjected to catastrophic tensile loading according to ASTM D 3039/D 3039M-95a for the determination of their residual mechanical properties (static strength, elastic modulus, failure strain).

3. RESULTS

3.1. Uninterrupted testing

3.1.1. Tensile testing

The stress-strain behaviour of the material under tensile loading was linear elastic up to failure, as is typical for the material under investigation [9]. The determination of the elastic modulus was performed by regression of the stress-strain data in the 0.1-0.3% strain range according to ASTM D 3039/D 3039M-95a.

Table 2 summarizes the static strength, σ_{ult}, elastic modulus, E, and failure strain, ε_{ult}, for each of the 12 specimens tested in tension along with the mode of failure as specified in ASTM D 3039/D 3039M-95a. The first character in this nomenclature signifies the type of failure (L corresponding to lateral failure and S to longitudinal splitting), the second character signifies the failure area (G corresponding to gauge) while the third character signifies the failure location (M corresponding to middle). The different modes of failure of the composite material under investigation are presented in the post-mortem pictures of indicative specimens in Fig. 3.

A simple frequency count of the values of static strength in Table 2 shows that 10 out of the total of 12 values vary around a common mean while two observations fall well below the rest. Then, the statistical strength of the material, calculated by

Table 2: Results of tensile testing: Properties of the composite materials

Specimen	Failure mode	σ_{ult}, MPa	E, GPa		ε_{ult}, %	
			strain gauge	**extensometer**	**strain gauge**	**extensometer**
tns-01	SGM	904	186.3 ± 0.5		0.50	
tns-02	SGM	1108	215.4 ± 0.4		0.52	
tns-03	LGM	1053	197.6 ± 0.4		0.53	
tns-04	SGM	996	211.6 ± 0.4		0.47	
tns-05	SGM	1198	211.3 ± 0.4		0.57	
tns-06	SGM	1138	208.1 ± 0.3		0.54	
tns-07	LGM	1253	221.1 ± 0.4	223.0 ± 2.1	0.56	0.54
tns-08	SGM	1118	220.5 ± 0.3	208.5 ± 0.4	0.50	0.52
tns-09	LGM	1172		197.8 ± 1.8		0.58
tns-10	LGM	1122	216.8 ± 0.3	183.8 ± 2.0	0.52	0.61
tns-11	LGM	1224	223.2 ± 0.3	214.0 ± 1.6	0.54	0.56
tns-12	LGM	1197		205.4 ± 1.1		0.58

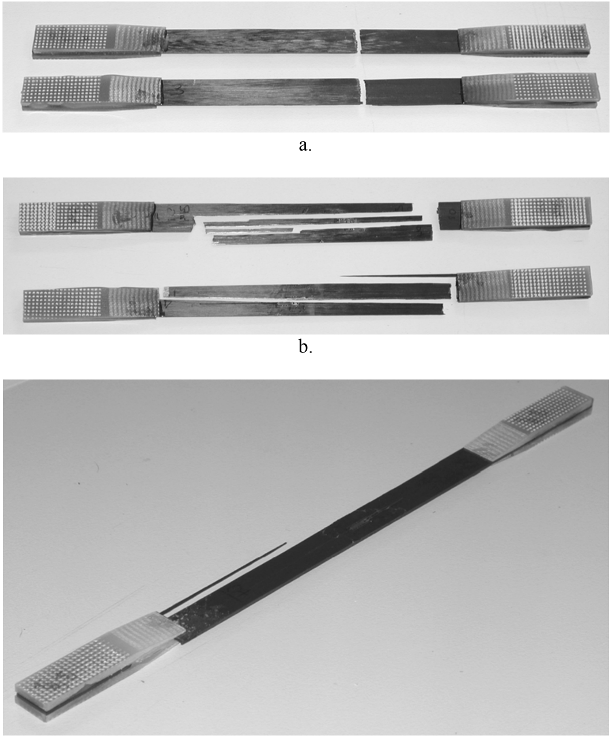

a. b. c.

Fig. 3: Indicative pictures of every mode of failure encountered during tensile testing of the specimens. (a) LGM, (b) SGM and (c) LIT (Lateral failure Inside Top grip)

excluding the 2 far-out points at 900-1000 MPa, is $\sigma_{ult(10)}$ = 1156 ± 61 MPa. The index "10"denotes the number of observations used for its calculation.

The elastic modulus of the composite was calculated as $E_{strg(8)}$ = 214.3 ± 8.4 GPa in experiments for which the strain was measured with a strain-gauge and as $E_{ext(6)}$ = 205.4 ± 13.5 GPa when the extensometer was employed for strain measurement. The statistical failure strain of the composite was $\varepsilon_{ult\ strg(8)}$ = 0.54 ± 0.02 % for strain-gauge measurements and $\varepsilon_{ult\ ext(6)}$ = 0.57 ± 0.03 % for extensometer measurements. As the indices in $E_{ext(6)}$ and $\varepsilon_{ult\ ext(6)}$ imply, the calculations of the elastic modulus and the failure strain for extensometer-aided experiments did not take into consideration the 2 far-out values corresponding in specimens tns-01 and tns-04, that were also excluded from the strength statistics.The difference noted in the calculated values of the elastic modulus and failure strain for the two strain-measurement techniques is a result of the different gauge length inherent to each method. While the gauge length of the strain gauge is $l_{g\ strg}$ = 5 mm, the corresponding length for the extensometer is 5 times larger, $l_{g\ ext}$ = 25 mm, hence justifying larger variations in recorded strain and modulus. To validate the compatibility of the findings using the 2 different strain measurement methods, the Student *t* test was employed [10]. The analysis showed the corresponding mean values not to differ significantly in the 0.05 significance level.

As far as the mode of failure is concerned, two equally preferable mechanisms where observed, Lateral failure in the Middle part of the Gage and longitudinal Splitting in the same location (LGM and SGM respectively). Six (6) of the specimens tested under tension failed in a brittle manner along a simple macrocrack perpendicular to the loading direction (LGM) while the remaining six (6) exhibited cracks along the loading and fibres direction (SGM).

3.1.2. Fatigue loading

The loading conditions, number of imposed cycles and mode of failure for the 14 specimens tested in fatigue loading are presented in Table 3. In this table, available values of residual properties (residual static strength, $\sigma_{ult\ resid}$, residual elastic modulus, E_{resid}, residual failure strain, $\varepsilon_{ult\ resid}$) are the results of catastrophic tensile testing of specimens that endured the noted number of cycles. It is important to retain the value of static strength used, $\sigma_{ult(10)}$ = 1156 ± 61 MPa, while σ_{max} corresponds to the maximum stress imposed by the loading cycle.

The S-N curve (load level vs. logarithmic number of cycles) of the fatigue tests is shown in Fig. 4. Specimens that endured 10^6 loading cycles are represented by right-arrowed symbols to signify that fatigue testing was interrupted to allow for catastrophic static –tensile- loading. Fig. 4 shows a clear influence of the load level to the fatigue life of the material. Specimens tested at load levels within the range of twofold standard deviation from the static strength, fail at random cycles while specimens tested below this level can endure more than 10^6 loading cycles. The example of specimen "ftg-13" is characteristic: this specimen endured 27438984 cycles at a load level of 0.80 without failing before the loading procedure was terminated manually and the specimen was subjected to tensile loading. As observed in Table 3, the specimen ultimately failed

Table 3: Loading conditions and properties of composite materials tested in fatigue. Also presented are the residual mechanical properties of specimens that endured 106 loading cycles.

Specimen	Failure Mode	Load level σ_{max} / σ_{ult}	Number of cycles	$\sigma_{ult\ resid}$ MPa	E_{resid} GPa strain gauge	E_{resid} GPa ext/meter	$\varepsilon_{ult\ resid}$ % strain gauge	$\varepsilon_{ult\ resid}$ % ext/meter
ftg-01	SGM	0.74	1506789	1352		228.7 ± 1.5		0.58
ftg-02	SGM	0.62	1152270	1290		224.5 ± 1.1		0.58
ftg-03	SGM	0.64	1260878	1252		222.0 ± 1.2		0.57
ftg-04	LGM	0.69	1057306	1073		221.6 ± 1.8		0.48
ftg-05	SGM	0.78	1050084	1226	220.6 ± 0.3		0.55	
ftg-06	LIT	0.83	1187706	950	223.8 ± 0.3		0.43	
ftg-07	SGM	0.87	1032238	1332	222.4 ± 0.3		0.59	
ftg-08	LGM	0.92	4284					
ftg-09	LIT	0.90	1370647	1306	232.7 ± 0.8		0.56	
ftg-10	LIT	0.91	59					
ftg-11	LGM	0.80	-	Premature failure				
ftg-12	SGM	0.90	96060					
ftg-13	SGM	0.80	**27438984**	1220	222.3 ± 0.1		0.54	
ftg-14	SGM	0.90	57082					

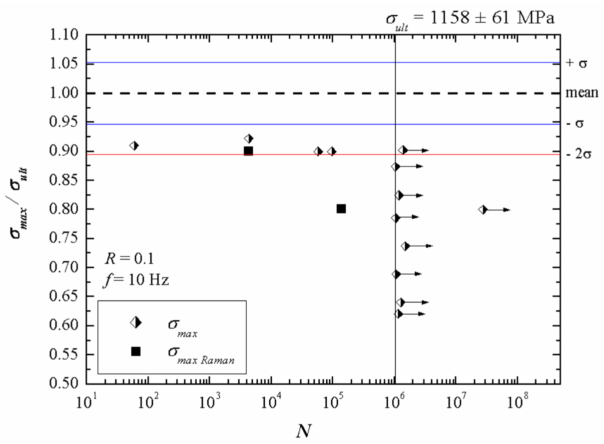

Fig. 4: S–N curve of the composite material tested in fatigue loading. Square symbols correspond to data from interrupted fatigue tests.

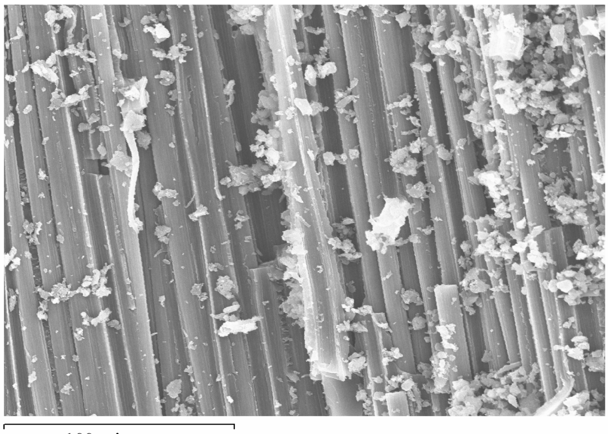

Fig. 5: SEM image of the fracture surface of specimen “ftg-13”. The intense presense of matrix debris is characteristic of the development of longitudinal cracks during fatigue loading.

in SGM mode, while SEM imaging of its fracture surface (Fig. 5) are characteristic of this mode of failure [11].

Based on the results in Table 3, it can be said that the fatigue performance of the investigated composite is compatible with the behaviour described in the past by Talreja [2], in all cases where the endurance fatigue limit of the matrix material of unidirectional polymer matrix composites appears at strain values larger that the failure strain of the composite. In this context, the S-N curve of the material does not exhibit gradual failures at consecutive load levels as a function of loading cycles, but rather a horizontal band of random failures at stress levels around the static strength below which specimens endure more than 106 loading cycles. For the composite material produced in this study, the value of endurance fatigue limit under the current loading configuration (R = 0.1 and f = 10 Hz) is approximately σ_{max} / σ_{ult} = 89.5 %

The representative stress-strain behaviour of fatigued post-fatigue specimen subjected to catastrophic static- tensile- loading for the determination of its tensile residual properties is presented in Fig. 6. The specimen endured 1050084 fatigue cycles at a load level of 0.78. The mechanical response of

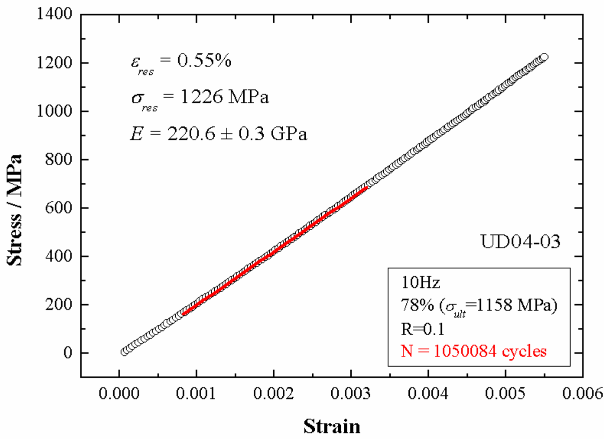

Fig. 6: Specimen “ftg-05” after 1050084 fatigue cycles at 0.78 load level: Typical linear elastic behaviour up to failure.

the specimen remained within the linear elastic regime up to failure. The determination of the elastic modulus was performed using the same procedure as mentioned previously.

Despite the different number of cycles imposed to the fatigued specimens, an attempt is made here to compare the residual post-fatigue tensile strength with that of the pristine composite material. In Fig. 7, the residual strength of 7 out of 9 fatigued specimens is shown to lie above the mean static strength of the pure tensile experiments ($\sigma_{ult(10)}$), with the exception of two data points falling well below the mean. Excluding the two far-out data at 950 and 1073 MPa, a

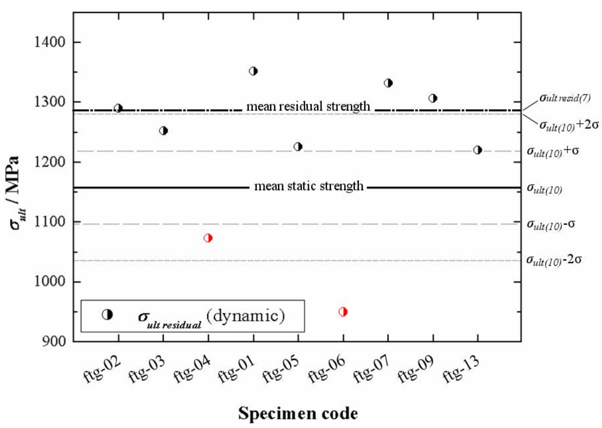

Fig. 7: The residual strength (and mean value $\sigma_{ult(7)}$, dash-dot line) of fatigued specimens plotted along with the mean static strength of the pure tension tests ($\sigma_{ult(10)}$, solid line) and its twofold standard deviation (dash lines). With the exception of two far-out values, the mean residual strength of the material is significantly larger than the mean static tensile strength.

mean residual strength, $\sigma_{ult\ resid(7)}$ value of 1282 MPa was calculated, and a Student *t* test at a 0.05 significance level proved that the values of the two populations differ significantly. This is a very important result for high modulus carbon fibre composites and has already been documented in the literature independently by Gamstedt [12] and Reifsnider [13]. It is attributed to a limited degree of debonding due to cyclic loading that results in the reduction of the stress concentration around a failed fibre within the debond length and the subsequent load redistribution to a larger number of fibres [12,13].

To validate the result of the residual elastic modulus and residual failure strain using the 2 different strain measurement methods, the Student *t* test was used and showed the corresponding mean values not to differ significantly in the 0.05 significance level. As far as the failure mode of the fatigued specimens is concerned, a clear preference in the SGM mode is noted, that involves the growth of cracks parallel to the longitudinal- fibre- axis of the specimen. Another 3 specimens failed within the gripped region while 3 specimens failure in LGM mode. By examination of the data in Table 3, it is evident that the LGM mode is associated with lower numbers of loading cycles, up to 4284, while, with the exception of one LIT failure, the rest of the specimens failed in SGM. This latter mode of failure is also observed in the greater part (6) of the specimens that endured 10^6 cycles and were subsequently subjected to tensile loading. These observations imply the formation and growth of “cracks” parallel to the loading- fibre- axis of the material during cyclic loading.

3.2. Interrupted testing

3.2.1. Interrupted tensile testing

Tensile tests were interrupted at consecutive strain levels for 24 hours as illustrated in Fig.8a. It is important to note that, common to the uninterrupted case, interrupted tensile tests were performed under crosshead displacement control, hence the specimen was held at constant displacement (strain) during interruption. Strain measurements were made by the use of strain gauges in this set of experiments.

Eight (8) specimens were subjected to interrupt

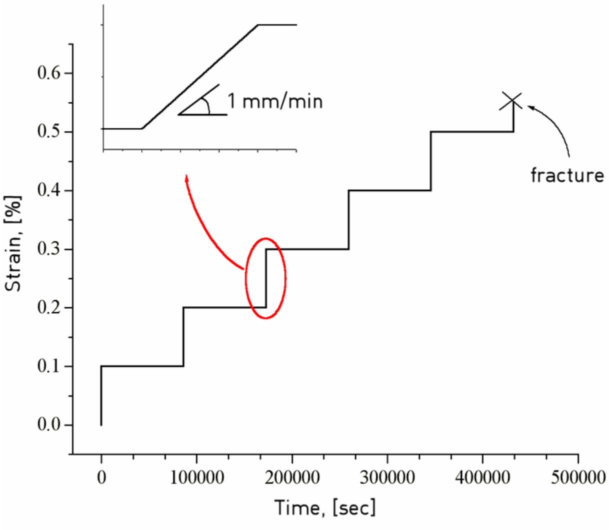

a

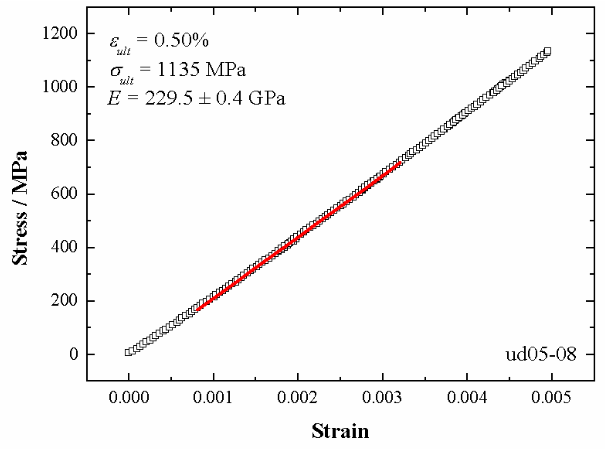

Fig. 9: Typical stress-strain behaviour of specimen "itns-08" under interrupted tensile testing.

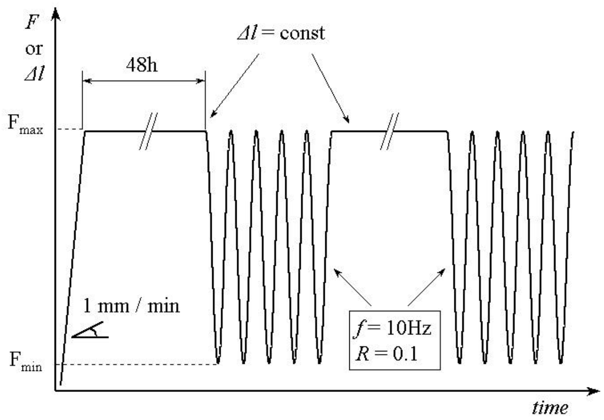

b.

Fig. 8: Loading flow and timescale of interrupted testing: a) tensile and b) fatigue loading.

tensile testing. The results of static strength, σult, elastic modulus, E, failure strain, εult, and mode of failure are summarized in Table 4 for each of the 8 specimens tested in interrupted tension.

Fig. 9 demonstrates the typical strain-strain behaviour of specimens tested under interrupted tension, along with the calculation of the elastic modulus using the same protocol as in uninterrupted testing. By examination of Fig 9, it is interesting to note that during testing interruptions, while displacement is held constant, no stress relaxation is noted in the material and the interruption locations cannot be "detected" in the stress-strain curves of the material. This effect owes most probably to the linear elastic nature of the material.

In Fig. 10, the values of static strength, elastic modulus and failure strain of specimens tested under interrupted tension are compared to the mean values of their counterparts from the uninterrupted tensile testing. As previously, the Student *t* test at a 0.05 significance level was employed to significane of the experimental findings. The values of all three investigated properties (σ_{ult}, E, ε_{ult}) were found to have remained practically unaffected due to interruptions in the loading procedure, with the means of each population pair being not significantly different. In contrast to the mechanical properties, the

Table 4: Results of interrupted tensile testing: Properties of the composite materials

Specimen	Failure mode	σ_{ult}, MPa	E, GPa strain gauge	ε_{ult}, % strain gauge
itns-01	SGM	1190	209.9 ± 0.4	0.56
itns-02	LGM	1089	208.8 ± 0.4	0.52
itns-03	LGM	1254	216.3 ± 0.3	0.57
itns-04	LGM	1214	218.2 ± 0.4	0.56
itns-05	LGM	1194	209.5 ± 0.3	0.56
itns-06	LGM	1027	209.7 ± 0.3	0.48
itns-07	SGM	1245	229.7 ± 0.3	0.54
itns-08	LGM	1135	229.5 ± 0.4	0.50

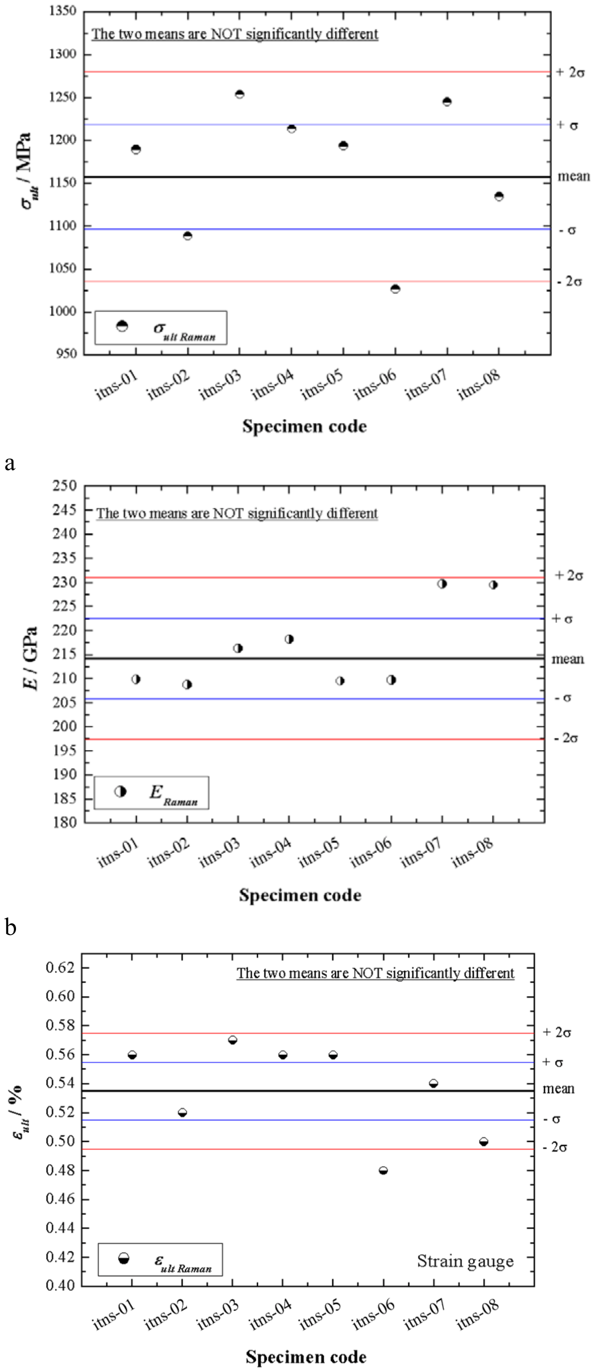

Fig. 10: Comparison of the properties of the composites under interrupted tensile testing with the statistical values of the uninterrupted tests (mean, standard deviation, twofold standard deviation): a. static strength, b. elastic modulus, c. failure strain. The properties remain unaffected by the interruption steps.

mode of failure in Table 4 appears to be affected by interrupted testing, with the LGM failure mode (6 specimens) being preferable over the SGM mode (2 specimens). It is then inferred that the combination of tension with prolonged residence time at different strain levels is presumably the factor that activates the LGM failure mode.

3.2.2. Interrupted fatigue tests

Interruptions of fatigue testing spanned time periods of 48 hours (Fig. 8b). Specimen “iftg-01” was tested at a load level of 0.90 and failed after 4168 cycles under the LGM mode. The same mode of failure was exhibited in specimen “iftg-02” that endured 136264 cycles at a load level of 0.80. In the S-N curve of the material, Fig. 4, the results of interrupted fatigue testing are presented as solid square symbols.

The unique mode of failure (LGM) of the specimens tested in interrupted fatigue indicates the degradation of fatigue life as a result of interrupted testing. Based on the findings of uninterrupted testing, specimen “iftg-02” should have failed in SGM mode after 136264 cycles, which was the only mode of failure recorded for specimens enduring more that 57000 cycles of uninterrupted fatigue. Prolonged residence at high loads can then induce the growth of pre-existing microcracks normal to the loading direction; a damage mechanism that can trigger LGM-compatible failure.

4. DISCUSSION

4.1 Effect of loading configuration on failure mode

The failure mode recorded for each specimen tested under the various loading configurations of the current work was used as a statistical measure to establish the role of loading configuration on type of failure. In Fig. 11, the number of specimens that failed under a specific loading configuration is plotted as a function of the corresponding failure mode. In this figure, the values of the axis “test type” are: “static” (corresponding to tensile loading), “stat_R” (corresponding to interrupted tensile loading), “dynamic” (corresponding to uninterrupted fatigue loading) and “dyn_R” (corresponding to interrupted fatigue loading). As shown, specimens tested in uninterrupted tensile loading did not show a preferable failure mode, with 6 specimens failing in LGM mode and an equal number of specimens failing in SGM. However, the scenario changes in the rest of the testing configurations. In uninterrupted fatigue testing, SGM (growth of cracks parallel to the loading axis) appears to be the preferable failure mode with

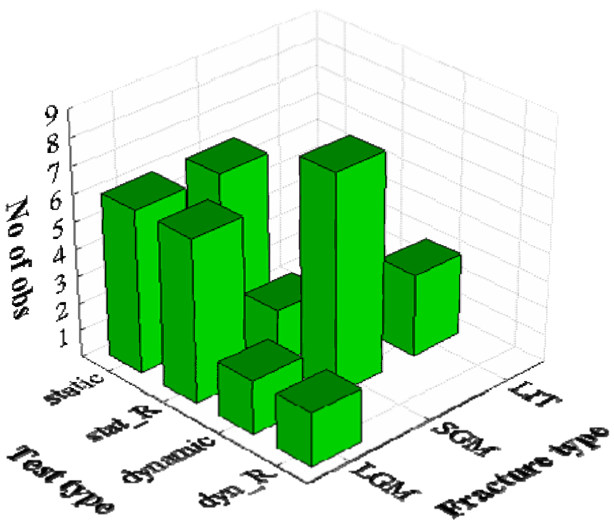

Fig. 11: 3-D representation of the number of specimens failing in various failure modes as a function of the testing configuration.

only 5 out of 13 specimens failing differently (LGM or LIT). Specimens tested in interrupted loading configurations show a clear tendency of failing according to LGM in which a single dominant macrocrack grows normal to the loading direction and the specimen fails abruptly. Not disregarding the small number of specimens tested in interrupted fatigue for a valid statistical comparison, this failure mode appears to remain uninfluenced by the loading configuration of the interrupted test (tensile or fatigue). It could then be inferred that, while fatigue appears to favour SGM failure in uninterrupted testing, the LGM mode dominates all interrupted tests. It is thus understood that interruptions in the loading procedure play a much more critical role in the determination of the failure mode than the loading configuration itself.

The preference of specimens loaded in uninterrupted fatigue, to fail according to the SGM mode can be rationalized based on the findings presented in section 3.1.2. The increase in static strength of the material after 10^6 loading cycles and the attribution of this effect to a certain degree of interfacial debonding as a result of cyclic loading [12,13] is indeed expected to cause the growth of cracks parallel to the axis of reinforcement of the material, which coincides here with the loading axis.

In contrary, the noted preference of specimens tested interruptedly in tension, as well as of the two tested in interrupted fatigue, to fail in LGM, indicates that during prolonged residence at the maximum loads, the pre-existing microcracks or flaws in the fibres evolve with time until a critical number of neighbouring fibres fail simultaneously to give growth to a dominant macrocrack normal to the loading direction. In the case of uninterrupted fatigue testing, the dimensions of such micro-flaws do not increase or increase slowly enough to give priority to the development of interfacial damage close to fibre discontinuities [12,13].

4.2 Indications of the effect of interrupted testing

Fatigue loading imposed on structural parts is seldom a purely cyclic sequence of alternating deformations or forces. In general, materials are expected to withstand a very wide and complex band of different load charges. The latter in combination with the fact that fatigue life is not a major parameter in structural design, has kept maximum design strains bound to 0.4% [14]. Within this regime, composite materials can withstand a great number of loading cycles without failing, with the damage developing under such conditions, not being a major problem in design. On the other hand, design criteria for composite materials will not unfold unless improved methodologies for prediction of their fatigue life are established. Key to this is the understanding of the various failure and damage mechanisms that develop and evolve during fatigue loading of these materials.

The interrupted fatigue loading scheme employed in this study is significantly more complex than conventional fatigue-testing protocols dictate, but is believed, to simulate real fatigue conditions much more closely than traditional schemes. In many applications, structures are not constantly loaded within an harmonically alternating load range, but fatigue is interrupted by other kinds of loadings, such as the residence at constant deformation of a certain period of time, as for example during resting of a landed airplane.

The results of interrupted testing indicate that the combined cyclic loading and residence at high loads for 48 hours scheme employed in this study, can trigger a premature fibre failure mechanism. The behaviour of specimen "iftg-02" is indicative: The specific specimen underwent the interrupted fatigue loading scheme to 80% of its static strength and failed after 136,264 cycles and 192 hours of residence at constant load (a total of 196 hours of combined loading), while at the same level of pure fatigue loading, specimen "ftg-14" withstood 2,743,984 cycles (762 hours of fatigue loading) without failing. It is important to note that, according to bibliographical records, epoxy resin / carbon fibre composite materials reinforced along the loading direction only do not exhibit creep [15,16] while the same holds for carbon fibres in air [17]. The observation of premature material failure indicates a probable deteriorative influence of consecutive interruptions of the fatigue loading procedure and prolonged residence at high loads on the fatigue life of the composite material under investigation. The appearance of such a damage mechanism as a result of interrupted fatigue loading appears a challenging objective to be independently investigated.

5. CONCLUSIONS

The current study investigated the mechanical performance of a Cf/epoxy laminate processed in autoclave environment. Coupon geometries of the composite material were tested under 4 different loading configurations: both pure and interrupted tension and fatigue. The static mechanical properties (static strength, elastic modulus and failure strain) and fatigue life parameters (S-N curve, endurance fatigue limit and residual properties) were obtained as the result of pure tensile and fatigue loadings. The statistical strength of the material was calculated as σ_{ult} = 1156 MPa while the elastic modulus as E = 210 GPa. The S-N curve of the material demonstrated that specimens tested at load levels lower than twofold standard deviation below the mean static strength of the composite, exhibit increased fatigue life, enduring more than 10^6 loading cycles. The latter finding was used to calculate the endurance fatigue limit of the material to $\sigma_{max} / \sigma_{ult}$ = 89.5 %. Specimens tested under interrupted tension and fatigue, failed abruptly after a single dominant macrocrack grew normal to the loading direction (LGM). Specimens loaded under pure fatigue conditions failed along cracks parallel to the loading axis (SGM) that appeared as a direct outcome of localized interfacial debonding effects. The interrupted fatigue loading scheme employed in this study, is believed to trigger premature fibre failure, hence deteriorating fatigue life of the material.

ACKNOWLEDGMENTS

The authors wish to thank Prof. Vassilis Kostopoulos of the Department of Mechanical Engineering and Aeronautics, University of Patras, Greece, for his valuable guidance throughout this work.

References:

1. Dauskardt RH, Ritchie RO and Cox BN (1993), Fatigue of Advanced Materials, *Adv Mater Processes,* **144**: 26-29
2. Talreja R (1987), Fatigue of Composite Materials, Technomic Publishing: Lancaster, Pennsylvania 17604, USA. ISBN 87762-516-6
3. Konur O and Matthews FL (1989), Effect of the Properties of the Constituents on the Fatigue Performance of Composites: A Review, *Composites* **20**:317–20
4. Melanitis N and Galiotis C (1993), Interfacial Micromechanics Using Laser Raman Spectroscopy, *Proc. of Royal Soc.-A*, **440**:379-398
5. Paipetis A and Galiotis C (1996), Effect of fibre sizing on the stress transfer efficiency in carbon/epoxy model composites, Composites A, 27: 755-767
6. Chohan V and Galiotis C (1997), Effects of Interface, Volume Fraction and Geometry upon Stress Re-Distribution in Polymer Composites under Tension, *Composites Science and Technology,* **57**:1089-1101
7. Koimtzoglou C, Kostopoulos V and Galiotis C (2002), Stress Transfer Efficiency in Model Composites Under Dynamic Loading, *Appl Phys A*, **76**:231-239
8. Koimtzoglou C, Dassios KG and Galiotis C, Acta Mater (2009), In Press, doi:10.1016/j.actamat. 2009.02.038
9. Smith PA (2000), Carbon Fiber Reinforced Plastics – Properties, in "Comprehensive Composite Materials", ed. A Kelly, C Zweben, Elsevier
10. Dally JW and Riley WF (1991), Experimental Stress

Analysis, 3rd ed., McGraw - Hill, Singapore
11. Hiley MJ (1999), Fractographic Study of the Static and Fatigue Failures in Polymer Composites, *Plas Rubb Comp*, **28**:210-227
12. Gamstedt EK (2000), Effect of Debonding and Fiber Strength Distribution on Fatigue-Damage Propagation in Carbon Fiber-Reinforced Epoxy, *J Appl Polym Sci*, **76**:457-474
13. Reifsnider KL (1994), Micromechanical Modeling of Polymer Composites, *Polymer*, **35**:5035-5040
14. Curtis PT and Davies AJ (2000), Fatigue Life Prediction Of Polymer Composites, Proceedings of the 9th European Conference on Composite Materials (ECCM-9), Brighton
15. Horoschenko A (1995), Beitrag zur Charakterisierung des Nichtlinear Thermoviskoelastischen Kriechverhaltens von Faserverbundwerkstoffen, PhD thesis, Technische Universitaet München
16. Peterman J and Schulte K (2002), The effects of creep and fatigue stress ratio on the long-term behaviour of angle-ply CFRP, *Comp Struct,* 57 205-210
17. Miyake T, Yamakawa T and Ohno N (1998), Measurement of stress relaxation in broken fibers embedded in epoxy using Raman spectroscopy, *J Mater Sci,* **33**:5177-5183

NOMECLATURE

Mechanical Properties

$\varepsilon_{ult\ strg}$	Failure strain of the composite measured via the "strain gauge" method
$\varepsilon_{ult\ ext}$	Failure strain of the composite measured via the "extensometer" method
ε_{ult}	Failure strain of the composite in interrupted testing (single strain measurement method by strain gauge)
$\varepsilon_{ult\ resid}$	Residual failure strain
σ_{ult}	Static strength of the composite
σ_{max}	Maximum stress value imposed by fatigue loading
$\sigma_{ult\ resid}$	Residual static strength
E_{strg}	Elastic modulus of the composite via the "strain gauge" method
E_{ext}	Elastic modulus of the composite via the "extensometer" method
E_{resid}	Residual elastic modulus
$property_{(number)}$	Statistical value of the property based on a limited number of equivalent observations within the same set (exclusion of specific observations)

Failure Modes

LGM	Lateral failure in the Middle part of the Gage
SGM	Longitudinal Splitting in the Middle part of the Gage
LIT	Lateral failure Inside the Top Grip/Tab

Experimental Properties

$l_{g\ strg}$	Gauge length of the strain gauge
$l_{g\ ext}$	Gauge length of the extensometer
N	Number of loading cycles in fatigue testing
R	Loading ratio (minimum/maximum applied load) in fatigue testing
f	Loading frequency in fatigue testing
σ	Standard deviation

Specimen codes

tns-	Specimen tested in tension
ftg-	Specimen tested in fatigue
itns-	Specimen tested in interrupted tension
iftg-	Specimen tested in interrupted fatigue